A Framework for Back-Analysis of 3D Rockfall Trajectories

Arnold Y. Xie[1(✉)], Zhanyu Huang[2], Thamer Yacoub[2], and Bing Q. Li[1]

[1] Department of Civil and Environmental Engineering, Western University, London, ON, Canada
arnold.xie@uwo.ca
[2] Rocscience Inc., Toronto, ON, Canada

Abstract. We define a novel normalized loss function to quantitatively evaluate the goodness-of-fit between simulated and measured rockfall trajectories using elapsed time and sampled rock positions. This loss function is optimized to back-analyze the coefficients of restitution R_n and R_t using a Monte-Carlo search of the parameter set $\theta = [R_n, R_t, v_0]$ where v_0 is the initial horizontal velocity. The trajectories are simulated assuming lumped mass rocks with initially horizontal projectiles and zero rotation. While our results are derived using position as the loss term, we note that our framework is entirely compatible with velocity or energy as a loss term as suggested by other researchers. The efficacy of the back-analysis framework is examined using synthetic and measured rockfall trajectories from a copper mine in British Columbia, Canada. The Monte Carlo search reveals significant non-uniqueness in the back-analyzed values of R_n and R_t, which can be mitigated by joint back-analysis that stacks the loss contour of multiple target trajectories. Parametric studies suggest that a minimum of 10,000 Monte Carlo samples should be simulated for an accurate solution, and that the spatial resolution of the topography is linearly correlated to the minimum loss. This measured trajectory was also used to test the viability of scaling R_n by velocity and mass. Our results suggest that velocity scaling performs similarly (12% deviation from measured path) to a static R_n value (9% deviation) while the measured trajectory cannot be satisfactorily reproduced (43% deviation) when scaling R_n by mass.

Keywords: Rockfall · parametric studies · back-analysis · Monte Carlo

1 Introduction

Rockfall hazard mitigation relies on estimates of their potential trajectories. Caviezel et al. [1] posits these trajectories are primarily controlled by the initial state of the projectile and its rock-slope interactions. There is significant uncertainty around the parametrization of these rock-slope interactions since laboratory test data are difficult to scale to the field [2]. Therefore, there is a need for tools to parameterize rockfall simulations using in-situ data. Full-scale induced rockfall experiments, where rock projectiles are manually cast from slopes of interest, can be used to measure the in-situ material properties and hence constrain rockfall simulators. Specifically, radar trackers [3] or

© The Author(s) 2023
R. E. Hammah et al. (Eds.): RIC 2023, AHE 19, pp. 806–819, 2023.
https://doi.org/10.2991/978-94-6463-258-3_75

imaging [4] can be employed to measure the trajectory of the induced rockfall event. One or multiple rockfall simulators can then be tuned to produce a modelled 2D or 3D trajectory that approximates the measured trajectory. This match can be defined on the basis of metrics such as bounce height, runout distance, and runout locations [5–7].

This procedure, where the model parameters and, in some cases, initial projectile state are adjusted to match the modelled trajectory with the measured one, is commonly termed back-analysis. Currently, these parameters are adjusted manually in small increments until the solution is qualitatively deemed sufficiently close [6]. This heuristic approach is particularly inherently limited for rockfall modelling which is non-smooth and non-unique owing to discrete impact events and sharp changes in topography. The present study proposed a framework to quantify the back-analysis procedure in terms of 1) the goodness-of-fit between a measured and modelled rockfall trajectory, and 2) a Monte Carlo search to determine how this goodness-of-fit varies with the coefficients of restitution.

2 Methodology

2.1 Rockfall Parametrization

We use the RocFall3 software v1.007 to simulate rockfall trajectories, where the primary inputs are the slope material properties, the mass and volume of the seeder (i.e. rock source), the initial position and velocity of the seeder, and the topography. Here, we back-analyze only for the material properties of the slope and the initial velocity of the seeder, given that the remaining inputs are assumed to be well constrained. Furthermore, we consider a lumped-mass generalization to reduce parameters of interest to the initial velocity (v_0) of seeders, and the normal and tangential coefficient of restitution (R_n & R_t) of the rock slope.

The coefficient of restitution (COR) in RocFall3 lumped-mass method describes the ratio of outbound to inbound velocity [8]. The normal COR (R_n) is the ratio of velocity components perpendicular to the slope surface at the impact point, while the tangential COR (R_t) denotes the ratio parallel to the slope surface. Due to energy dissipation, the velocity decreases after each bounce resulting in an outbound velocity lower than the inbound one. Hence, we allow R_n and R_t to vary uniformly in the range [0, 1]. The initial speed (v_0) is a scalar denoting the magnitude of the cast-out velocity of a seeder and cannot be assumed to be zero for rockfall experiments where rocks are manually cast from a slope. The direction of cast-out velocity is defined by trend and dip. The trend is set based on the initial measured trajectory. The dip is set to 0 assuming a horizontally launched projectile. We assume zero initial rotation.

In this work, we include two types of datasets: measured paths and synthetic paths. The measured paths are trajectories measured by radar trackers from IDS GeoRadar on real slopes. They demonstrate the applicability of the framework. However, it is challenging to explore the accuracy of the workflow with measured paths since we do not know the true values of R_n and R_t. Thus, we introduce synthetic paths which take a simulated trajectory as the target trajectory to be matched by the back-analysis. They facilitate parametric investigation of the accuracy and precision of our framework under a range of conditions.

2.2 Loss Function

The key question for back-analysis is to quantitively define a 'good match' between a measured trajectory and its corresponding modelled trajectory. We quantify the difference using a loss function expressed in Eq. (1). In the equation, x and y are the coordinates of a target sampled location along the rockfall trajectory in a local cartesian coordinate system. The y-axis is aligned with north. The hatted variables $\hat{x}, \hat{y}$ denote a modelled sampled location along the modelled rockfall trajectory in the same local co-ordinate system. The t denotes the time stamp of a sampled location, hence, $(x, y)_t$ denotes the location of the rock at time step t. The operator $||\ldots||$ returns the distance between the two given locations. Note that elevations are not generally well constrained by radar tracking and may differ from the modelled topography - they are therefore not considered in the present study. Each misfit vector is defined from sample points on the target trajectory and to the modelled sample point with closest time stamp. The misfit vectors are depicted as orange arrows in Fig. 1. We sum the magnitude of all misfit vectors to obtain a single value of total misfit denoted as the loss between a measured and a modelled path. The loss is then normalized by the total travel distance of the target trajectory to avoid bias against longer trajectories. The k in the denominator denotes the k-th sample location as a variable to iterate through all target sample locations along the measured rockfall trajectory.

$$Loss\left(x, y, \hat{x}, \hat{y}, t\right) = \frac{\sum_{t=0}^{N} ||(x, y)_t, \left(\hat{x}, \hat{y}\right)_t||}{\sum_{k=2}^{N} ||(x, y)_k, (x, y)_{k-1}||} \tag{1}$$

A target sample location may match multiple modelled sample locations as shown by the last sample location in Fig. 1. This usually occurs at the last target location when the modelled trajectory has a longer duration than the target trajectory. Conversely, the last location of the modelled trajectory may match multiple target locations if the modelled trajectory has shorter duration than the target path. This feature penalizes modelled trajectories with either too short or too long durations.

Finally, we conduct a Monte Carlo search of the parameter set $\theta = [v_0, R_n, R_t]$ and denote the optimal back-analyzed parameter set θ^* as those with lowest loss. The following sections describe the details of this optimization using synthetic paths and then measured rockfall trajectories from an open pit mine in British Columbia (BC), Canada.

3 Back-Analysis of Synthetic Trajectories

We first explore the applicability of the loss function and parameter search on synthetic datasets generated from a high-resolution open-pit mine topography. Details of the topography can be found in Tutorial 1 from the Rocfall3 manual [9].

We assign the slope material to limestone with $R_n = 0.315$, $R_t = 0.712$. Next, we cast 5 seeders and assign their trajectories as target synthetic trajectories. The cast-out locations of the 5 target seeders are shown in Fig. 2. They are placed at representative locations around the pit, including a steep slope, a shallow slope, and corners. These

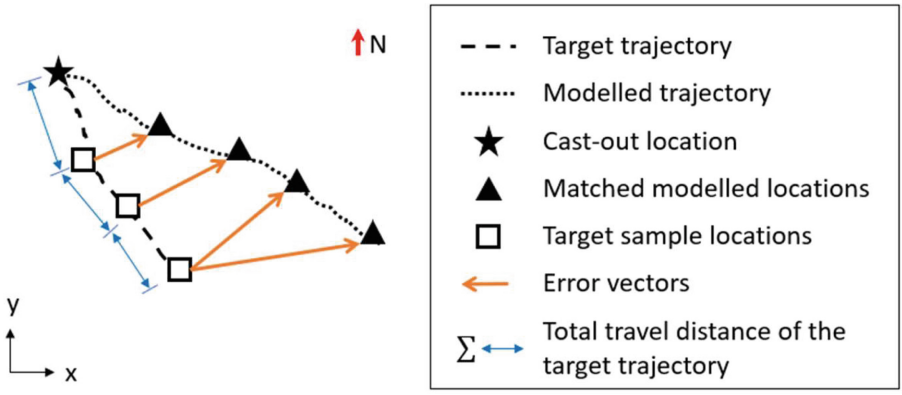

Fig. 1. Schematic plot for loss function. Loss is the summation of the magnitude of misfit vectors normalized by the total travel distance of the target trajectory. The modelled locations are matched to the target locations on the basis of time elapsed since the start of the rockfall event

locations are intended to test our framework against a range of potential rockfall trajectories. All seeders are assigned initial velocity directions towards the pit as indicated in Table 1. Figure 3a illustrates the rockfall path corresponding to Seeder#2, which serves as the target trajectory for results discussed in Sects. 3.1 and 3.2. Seeders are additionally assigned the following parameters:

- weight of 1000kg, density of 2.7 ton/m^3
- placed 5 m above the slope surface
- initial speed 1.5 m/s in horizontal direction without any rotation

Figure 3b shows the range of modelled trajectories generated in the process of our Monte Carlo search of the parameter set $\theta = [v_0, R_n, R_t]$. We use uniform distributions as we have limited a priori information, specifically $v_0 \in [0, 5]$ m/s, $R_n \in [0, 1]$, $R_t \in [0, 1]$.

Simulations are performed on a Windows workstation with 64GB RAM, and a core i9-12900K processor. No graphic processing unit is involved.

Sections 3.1 and 3.2 explore the effect of the number of Monte Carlo samples and the effect of the topography resolution respectively. In each case, the dependent variable is the loss defined by Eq. (1). Increasing the number of modelled trajectories can improve the accuracy of the optimum solution but requires more computation. Profiling the minimum loss over the number of modelled trajectories give us a preliminary estimation on the random search efficiency. The topography resolution is an open question for any task involving remote sensing. Its impact is more significant for back-analysis since one must digitize the topography at a finite resolution. To investigate the importance of topography resolution, we down-sample the topography to a range of resolutions and measure the degree of misfit at each resolution using Eq. (1).

Sections 3.1 and 3.2 demonstrate that the back-analysis can be highly non-unique [10]. To overcome this limitation, we demonstrate that summing the loss from multiple target trajectories at the same site can return a more reliable estimation on R_n and R_t.

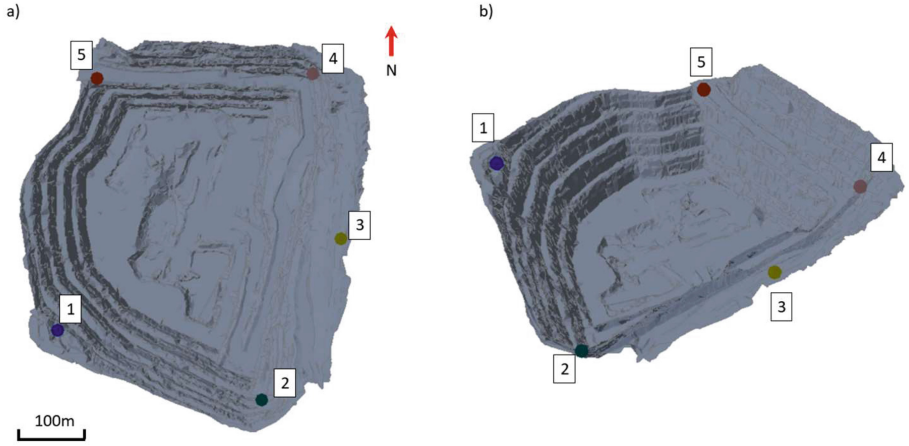

Fig. 2. Illustration of the 5 seeder locations for the synthetic dataset in a) plan view and b) oblique view. Seeders are placed 5 m above the slope surface. Seeder#2 is discussed in Sects. 3.1 and 3.2. Other seeders are discussed in Sect. 3.3

Table 1. Summary of setup and back-analysis of the 5 target trajectories, together with stacked optimal fit and true v_0, R_n, R_t values

Seeders#	Trend(deg)	Back-analyzed parameter set θ*		
		v_0	R_n	R_t
1	45	1.488	0.30	0.77
2	0	1.581	0.32	0.69
3	270	1.543	0.30	0.70
4	225	1.417	0.32	0.75
5	135	1.507	0.34	0.63
Stacked	–	–	0.29	0.77
θ_{true}	–	1.500	0.315	0.712

3.1 Number of Seeders

To explore the number of required samples for the Monte Carlo search, we conduct 5 back-analyses with 50,000, 25,000, 10,000, 5,000, and 1,000 modelled trajectories. These simulations share a common target trajectory denoted as Seeder#2 in Fig. 2 with parameter set θ_{true} indicated in Table 1. Figure 4 depicts the loss calculated by Eq. 1 from various realizations of $\theta = [R_n, R_t, v_0]$.

Note that we visualize the reconstructed loss contour on the R_n-R_t plane with loss expressed by color intensity since the coefficients of restitution are the primary outcomes of the back-analysis. It is only necessary to vary v_0 in the Monte Carlo search because the true initial velocity is difficult to measure in the field since the radar instruments are sparsely sampled in time. Moreover, the grainy pattern allows us to evaluate the

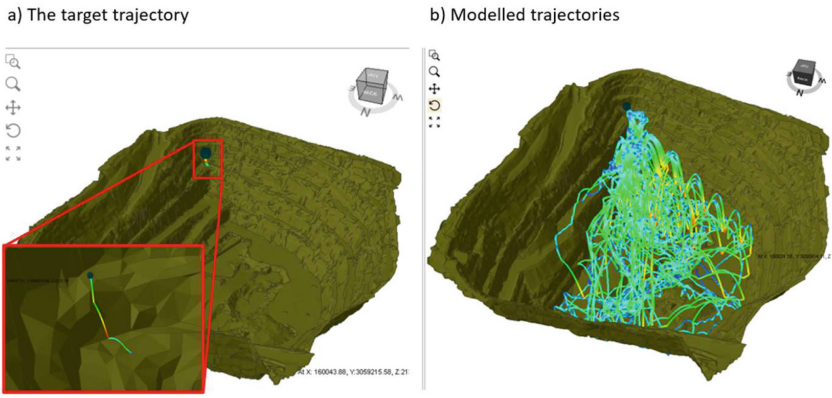

Fig. 3. Illustration of trajectories generated by seeder#2 with a) the single target trajectory and b) modelled trajectories using a Monte Carlo search. The color of trajectory indicates instantaneous speed. Blue is low speed, and red is high speed. Each modelled trajectory is simulated using a randomly drawn set of $\theta = [R_n, R_t, v_0]$

uncertainty of loss value over the varying initial speed. For instance, Fig. 4a exhibits a diagonal region of decreased loss and a relatively consistent color pattern at the upper left corner, i.e., lower uncertainty in this region. The diagonal region of decreased loss spreads out at the lower right end, which indicates the loss becomes more unstable. Meanwhile, the lower triangular region is more stable in terms of loss. It implies that loss varies less when R_t is less than half of R_n. The modelled trajectories using these values of R_n and R_t may not be able to gain enough outbound normal speed and stop in the vicinity of their first impact location. The misfit of these trajectories consists mainly of the penalty on total distance. The upper triangular region, on the other hand, exhibits predominantly high loss over 0.6. Trajectories in this region exhibit unrealistically long runout distances.

The diagonal region of low loss appears in all contours regardless of the number of trajectories, indicating a range of $\theta = [R_n, R_t, v_0]$ that all produce approximately the same trajectory as the target. However, the resolution of the loss contour improves with the number of Monte Carlo samples but does not fully resolve the issue of non-uniqueness in the solution space. The dark and bright patches in Fig. 4e are larger than Fig. 4a while the locations of the patches are similar.

Figure 5 depicts how the number of Monte Carlo samples affects the optimum parameter set $\theta^* = [R_n^*, R_t^*, v_0^*]$ and corresponding minimum loss. All 4 parameters become more stable when there are more than 10,000 samples. The minimum loss decreases exponentially with increasing number of seeders. v_0 varies from 1.4 m/s to 1.9 m/s, which only comprises 10% of the entire assigned search range of 5 m/s. We conservatively simulate 50,000 samples for subsequent back-analyses, which is by our computational capacity. The loss is expected to further improve with more samples and would also benefit from a more sophisticated optimization strategy.

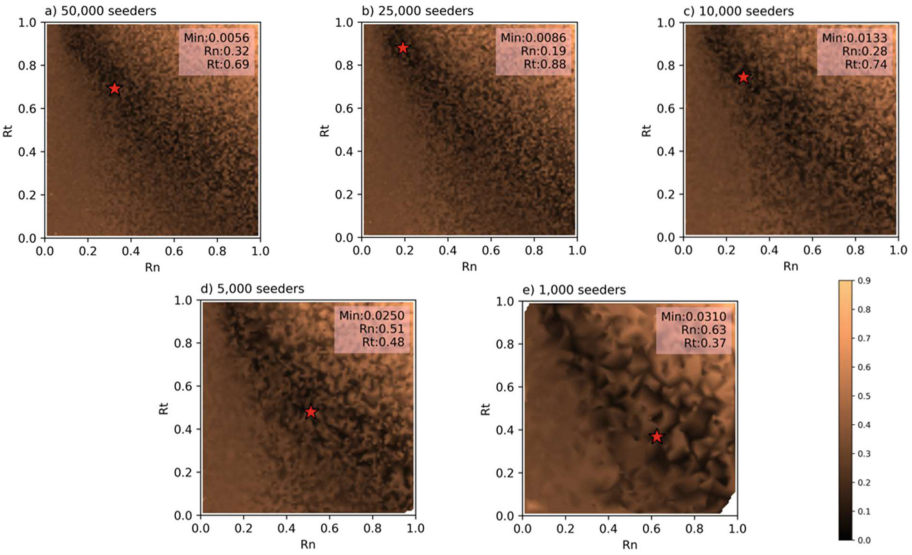

Fig. 4. Loss contour at different number of Monte Carlo simulations. Darker color indicates lower loss (better fit between target and back-analyzed trajectory). The red star marks out the minimum loss. The irregular dark patches are caused by stacking results at various initial velocities

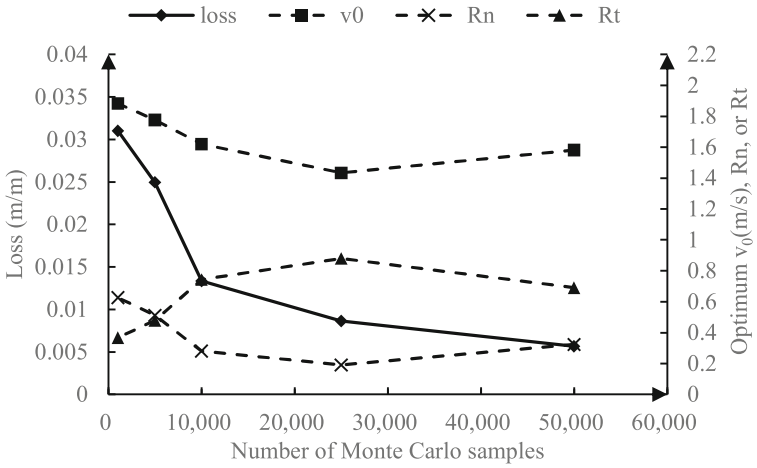

Fig. 5. The minimum loss (loss) plotted on left ordinate and corresponding optimum initial velocity (v_0), normal coefficient of restitution (R_n), and tangential coefficient of restitution (R_t) on right ordinate over the number of Monte Carlo samples

3.2 Topography Resolution

Here, we conduct the back-analysis of seeder#2's trajectory at 100%, 50%, 20%, 10% of the original topography resolution to explore how the quality of the digital elevation model affects the quality of rockfall trajectory back-analysis. Figure 6 shows the loss

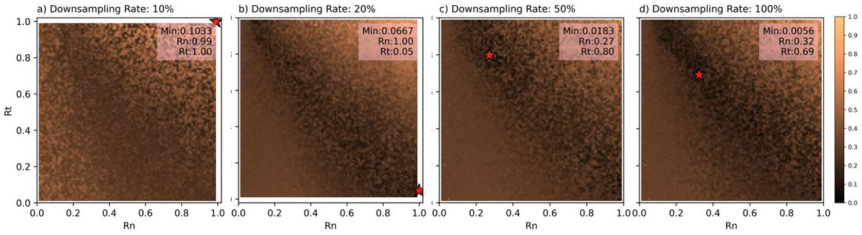

Fig. 6. The loss contour at down sampling rate a) 10% b) 20% c) 50% d) 100% with minimum loss indicated by the red star. R_n and R_t are uniformly simulated between 0 and 1. Initial velocity v_0 ranges from 0 to 5 m/s. 50,000 Monte Carlo simulations are shown in each panel

contour at these down-sampling rates. The diagonal region of decreased loss becomes less pronounced as the topography resolution decreases. The minimum loss value also decreases with decreasing resolution, i.e. poor topography resolution reduces our ability to back-analyze the target trajectory. The upper triangular region, on the contrary, does not change significantly. Trajectories modelled using high values of R_n and R_t feature fewer rock-slope interactions and so are less sensitive to topography resolution. Consequently, the deviation between the best modelled and target trajectories increases when topography resolution decreases. It is noteworthy that minimum loss is found at the boundary of the search space at 10% and 20% resolution as shown in Fig. 6a and b. Figure 6a supports the assertion that minimizing rock-slope interaction at a low-resolution topography approximates the target path. Figure 6b shows the best fit at zero R_t but 100% normal restitution, i.e., the tangential velocity is zeroed after each impact but no velocity dissipation occurs in the normal direction. The trajectory is terminated once the angle between the inbound velocity and slope is too small. This is an apparent violation of physics and highlights the importance of topography resolution in 3D geomechanical modelling.

We express the down sampling rate as an equivalent grid spacing by assuming the triangular grid is evenly distributed and treating the area of 2 triangles as a unit square grid. Figure 7 illustrates the minimum loss increases linearly with decreasing grid resolution. The points on the x-axis from left to right corresponds to 100%, 50%, 20%, 10% down sampled topography.

3.3 Joint Back-Analysis Using Multiple Target Trajectories

The loss contours presented in Fig. 4 and Fig. 6 suggest significant non-uniqueness in the back-analysis, i.e. a range of $\theta = [R_n, R_t, v_0]$ can all produce a similar trajectory to the target. This can also be seen in Table 1, where the optimal v_0 is larger than the true value for seeder#2 and seeder#4. This non-uniqueness can be mitigated by stacking (summing) the loss contours from multiple measured trajectories, i.e. we jointly back-analyze R_n and R_t using target trajectories from all 5 seeders shown in Fig. 2, rather than only relying on a single trajectory. This is shown in Fig. 8, which includes the mean loss contour from all 5 target trajectories alongside the loss contour from the individual target trajectories. Note that we plot the loss function at $v_0 = 1.5$m/s to better visualize the optimum solution. Overall, Fig. 8f) exhibits a smaller region of low loss than the

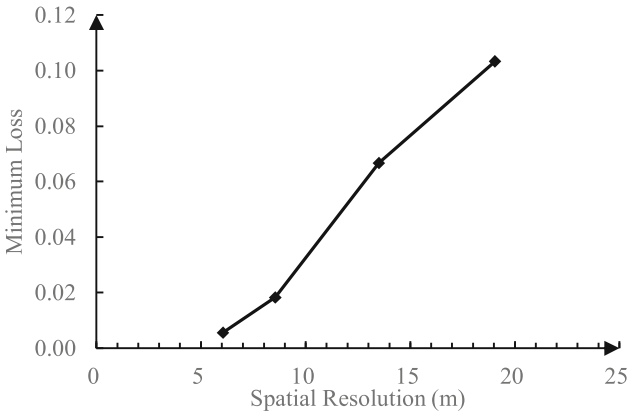

Fig. 7. Minimum loss at each spatial resolution. Lower values imply better spatial resolution

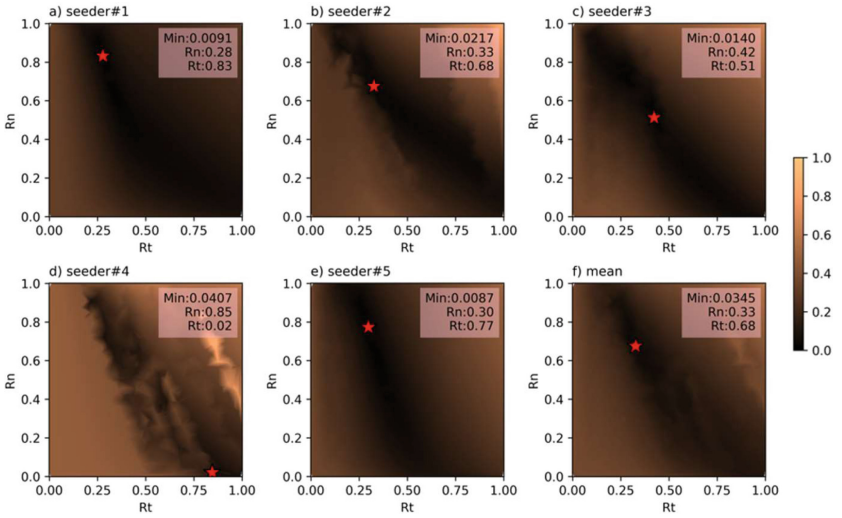

Fig. 8. R_n R_t loss contour at initial speed of 1.5 m/s for back-analysis of Seeder#1 to #5. Panel f) shows the mean of panels a)-e)

loss contours of individual trajectories as seen in Fig. 8a - e, reflecting a higher degree of confidence in the optimal solution set.

4 Back-Analysis of Rockfall Trajectory Measured at an Open-Pit Mine in BC, Canada

Here we demonstrate the efficacy of our back-analysis framework using a rockfall trajectory measured using a radar tracker at a copper open pit mine in British Columbia, Canada. The rock slope consists primarily of bornite and calcite, and the topography is

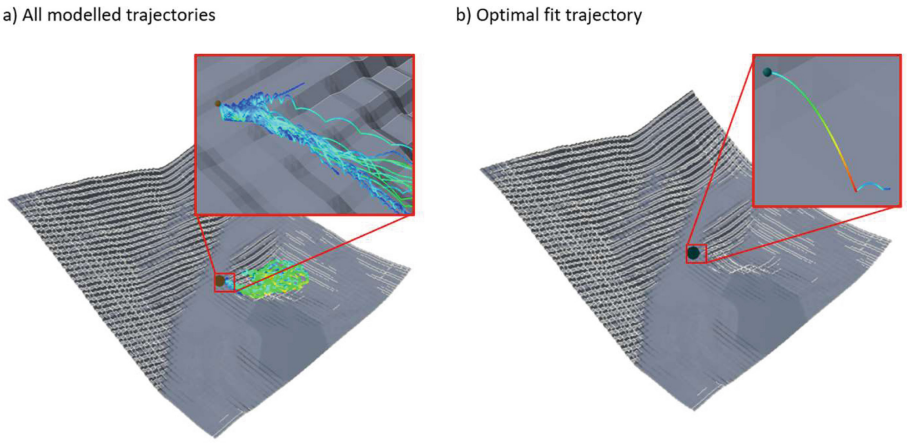

Fig. 9. Back-analysis of a rockfall trajectory measured at an open-pit mine in BC. a) all Monte Carlo sampled modelled trajectories, b) best-fit back-analyzed trajectory

obtained from the native Rocfall3 terrain generator. The back-analysis framework is the same as with the synthetic dataset except that the target trajectory is measured in the field and thus the true values of $\theta_{true} = [v_0, R_n, R_t]$ are unknown. The pit and back-analyzed rockfall trajectory are shown in Fig. 9. Figure 9a shows all modelled trajectories generated through the Monte Carlo search. The majority of the modelled rockfall events runout to the bottom of the pit. The measured and optimal trajectory shown in Fig. 9b arrests prior to the crest of the bench, which presents a discrete constraint for the back-analysis.

4.1 Results

Figure 10a depicts the loss contour derived from 50,000 Monte Carlo samples of modelled trajectories. An offset diagonal region of low loss separates the contour into 2 parts. The lower left occupies a larger area, where loss generally ranges from 0.4 to 0.6. Conversely, the upper right corner predominantly comprises trajectories with loss over 0.7 as illustrated by a bright color pattern. The region of low loss is located closer to the upper right corner compared with that in the synthetic dataset. It implies the measured trajectory has more inertia than the simulated target trajectories. Thus, the low loss trajectories reflect scenarios where most of the energy is retained after each impact, i.e., higher R_n and R_t.

The best fit is obtained at $R_n = 0.90$ and $R_t = 0.63$. Figure 10b portrays a plan view of the measured and optimal back-analyzed modelled trajectories. The first 3 sampled points from the modelled path aligns well with the measured path but diverges from the 4th sampled point. Since the tracker measures rock position at regular intervals, the increasing distance between adjacent points indicates the measured rock is accelerating while traveling from $X_{rel} = 10$m to $X_{rel} = 40$m. The modelled trajectory is again consistent with the measured locations at the end of the rockfall trajectory. We suspect that this mismatch during the middle of the trajectory can be attributed to limited topography resolution, which is supported by the 'crossmatch' labeled by the blue arrow in Fig. 10b.

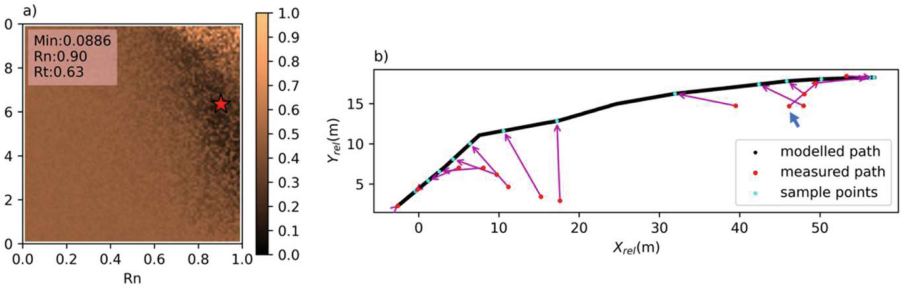

Fig. 10. Back-analysis of a rockfall trajectory measured at an open-pit mine in BC. a) loss contour with respect to R_n and R_t at any v_0. Star marks the minimum loss b) plan view of measured and best-fit modelled trajectories. The cyan points represent locations utilized in loss calculation. Magenta arrows visualize the misfit vectors. X_{rel} and Y_{rel} denotes the local cartesian coordinate system. The blue arrow in b) highlights an intriguing 'crossmatch' potentially resulting from limited topography resolution

4.2 Velocity and Mass Dependency of R_n

Pfeiffer and Bowen [11] suggested that the normal coefficient of restitution (R_n) should be scaled according to the instantaneous speed at the impact or mass of the rock. The former is denoted as Velocity damping expressed by Eq. (2), where V_{rock} denotes the speed at the impact and the scaling factor $K = 9.144$. The latter is denoted as Mass damping expressed by Eq. (3), where M_{rock} denotes the mass of the rock and the scaling factor $C = 1000$.

$$R_n'(Velocity) = \frac{R_n}{\left(1 + (V_{rock}/K)^2\right)}; K = 9.144 \tag{2}$$

$$R_n'(Mass) = \frac{R_n}{\left(1 + (M_{rock}/C)^2\right)}; C = 1000 \tag{3}$$

Here, we explore whether these scaling factors improve the back-analysis of the measured rockfall trajectory. We set $v_0 = 3.17$ m/s according to the previous analysis to reduce the number of free parameters and accordingly reduce the number of Monte Carlo samples to 5,000. We show the most representative trajectories in Fig. 11 among the top 3 fits. We see that the velocity scaling (Fig. 11b) results in a slightly worse-fitting modelled trajectory compared to a static R_n (Fig. 11a), and that the simulator is unable to produce a realistic rockfall trajectory using mass scaling (Fig. 11c).

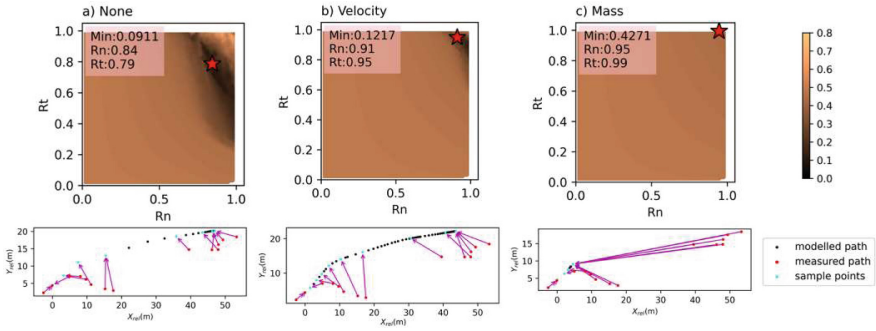

Fig. 11. Back-analysis of the measured trajectory shown in Fig. 10 using a) static R_n value b) velocity-scaled R_n, and c) mass-scaled R_n with loss contours and plan views of trajectories simulated by the annotated parameter sets. The star and annotation refer to the 3rd best-fit

5 Conclusion

We define a new normalized loss function to quantitatively evaluate the goodness-of-fit between simulated and measured rockfall trajectories using elapsed time and sampled rock positions. This loss function is optimized to back-analyze the coefficients of restitution R_n and R_t using a Monte-Carlo search of the parameter set $\theta = [R_n, R_t, v_0]$. The trajectories are simulated assuming lumped mass rocks with initially horizontal projectiles and zero rotation. While our results are derived using position as the loss term, we note that our framework is entirely compatible with velocity or energy as a loss term as suggested by other researchers.

The efficacy of the back-analysis framework is examined using synthetic and measured rockfall trajectories from a copper mine in BC. The Monte Carlo search reveals significant non-uniqueness in the back-analyzed values of R_n and R_t, which can be mitigated by joint back-analysis that stacks the loss contour of multiple target trajectories. Parametric studies suggest that the number of Monte Carlo samples is critical to obtain an accurate solution, which depends on the specific topography of interest. Additionally, we find the spatial resolution of the topography is linearly correlated to the minimum loss. Our methodology satisfactorily reproduces a rockfall trajectory measured using a radar tracker at a copper mine in BC. This measured trajectory was also used to test the viability of scaling R_n by velocity and mass. Our results suggest that velocity scaling performs similarly to a static Rn value while the measured trajectory cannot be reproduced when scaling Rn by mass.

We note two major limitations to the proposed method. Firstly, the Monte Carlo search strategy is computationally expensive, and the method would benefit from a more efficient optimizer. Secondly, the proposed method does not attribute an uncertainty to the optimal parameter set – as always it is the responsibility of the engineer to qualitatively verify the similarity of the modelled and measured trajectories, and whether the inverted parameters are reasonable.

Acknowledgements. The research presented in this paper was supported by NSERC Alliance Grant # 576858 in partnership with Rocscience Inc. The authors would like to express their sincere

gratitude for this support. We would also like to thank two anonymous reviewers for their valuable feedback.

References

1. Caviezel, A., Ringenbach, A., Demmel, S.E., Dinneen, C.E., Krebs, N., Bühler, Y., Christen, M., Meyrat, G., Stoffel, A., Hafner, E., Eberhard, L.A., von Rickenbach, D., Simmler, K., Mayer, P., Niklaus, P.S., Birchler, T., Aebi, T., Cavigelli, L., Schaffner, M., Rickli, S., Schnetzler, C., Magno, M., Benini, L., Bartelt, P. The relevance of rock shape over mass—implications for rockfall hazard assessments. Nature Communications 12(1) 5546 (2021).
2. Li, L., Lan, H. Probabilistic modeling of rockfall trajectories: a review. Bull Eng Geol Environ 74, 1163–1176 (2015). https://doi.org/10.1007/s10064-015-0718-9.
3. Miller, P.K., Vessely, M., Olson, L.D., Tinkey, Y. Slope stability and rock-fall monitoring with a remote interferometric radar system. In Geo-Congress 2013: Stability and Performance of Slopes and Embankments III, pp. 304–318 (2013).
4. Noël, F., Jaboyedoff, M., Caviezel, A., Hibert, C., Bourrier, F. and Malet, J.-P. Rockfall trajectory reconstruction: a flexible method utilizing video footage and high-resolution terrain models." Earth Surface Dynamics 10(6), 1141–1164 (2022).
5. Wyllie, D. C. Calibration of rock fall modeling parameters. International Journal of Rock Mechanics and Mining Sciences, 67, 170–180 (2014).
6. Mateos, R.M., García-Moreno, I., Reichenbach, P., Herrera, G., Sarro, R., Rius, J., Aguiló, R., Fiorucci, F. Calibration and validation of rockfall modelling at regional scale: application along a roadway in Mallorca (Spain) and organization of its management. Landslides. 13:751–763 (2016).
7. Kim, D. H., Gratchev, I., Berends, J., Balasubramaniam, A. Calibration of restitution coefficients using rockfall simulations based on 3D photogrammetry model: a case study. Natural Hazards, 78, 1931–1946 (2015).
8. Stevens, W.D. RocFall, a tool for probabilistic analysis, design of remedial measures and prediction of rockfalls. Diss. (Doctoral dissertation) (1998).
9. RocFall3 Tutorial, https://www.rocscience.com/help/rocfall3/tutorials/tutorials-overview/getting-started-tutorial, last accessed 2023/02/11.
10. Walton, G., Sinha, S. Challenges associated with numerical back analysis in rock mechanics. Journal of Rock Mechanics and Geotechnical Engineering (2022).
11. Pfeiffer, T. J., & Bowen, T. D. Computer simulation of rockfalls. Bulletin of the association of Engineering Geologists, 26(1), 135–146 (1989).

Open Access This chapter is licensed under the terms of the Creative Commons Attribution-NonCommercial 4.0 International License (http://creativecommons.org/licenses/by-nc/4.0/), which permits any noncommercial use, sharing, adaptation, distribution and reproduction in any medium or format, as long as you give appropriate credit to the original author(s) and the source, provide a link to the Creative Commons license and indicate if changes were made.

The images or other third party material in this chapter are included in the chapter's Creative Commons license, unless indicated otherwise in a credit line to the material. If material is not included in the chapter's Creative Commons license and your intended use is not permitted by statutory regulation or exceeds the permitted use, you will need to obtain permission directly from the copyright holder.